

Studying Λ interactions in nuclear matter with the $^{208}\text{Pb}(e,e'\text{K}^+)^{208}\text{Tl}$ reaction

Letter of Intent submitted to the Jefferson Lab PAC...

O. Benhar¹, F. Garibaldi^{1*}, T. Gogami³, E.C. Markowitz², S.N. Nakamura³, J.Reinhold², L. Tang^{4,5},
G.M. Urciuoli¹, I.Vidana⁶

1Istituto Nazionale di Fisica Nucleare, Sezione di Roma, P. A. Moro Rome, Italy

2Florida International University, Miami, Florida 33199, USA

3Department of Physics, Graduate School of Science, Tohoku University, Sendai, 980-8578, Japan

4Thomas Jefferson National Accelerator Facility, Newport News, Virginia 23606, USA

5Department of Physics, Hampton University, Hampton, Virginia, 23668, USA

6Istituto Nazionale di Fisica Nucleare, Sezione di Catania, Catania, Italy

* Contact person

1. Introduction.

An ambitious and challenging experimental program, aimed at obtaining high-resolution hypernuclear spectroscopy via the $(e,e'\text{K}^+)$ reaction, was started at Jefferson Lab 15 years ago. The data, taken in both Hall A and Hall C using p-shell and medium-mass nuclear targets, have provided clear spectra with 0.5~0.8-MeV energy resolution. The process, whose feasibility has been established at JLab, is now widely recognized as a powerful tool to study hypernuclear spectroscopy, in addition to the (K^-, π^-) and (π^+, K^+) reactions. Electron- and hadron-induced reactions are in fact complementary to one another, being predominantly driven by spin-flip and non-spin-flip mechanisms, respectively. Furthermore, the $(e,e'\text{K}^+)$ reaction allows for a much better energy resolution and produces mirror hypernuclei with respect to those produced with hadron probes. The 6 GeV experiments provided the experience needed to confidently set up a new program for the 12 GeV era.

The JLab hypernuclear collaboration proposed to PAC44 a coherent series of studies of the $(e,e'\text{K}^+)$ reaction, to be performed using targets spanning a wide range of mass. The purpose of this analysis was investigation of the ΛN interactions in a variety of nuclear media. The PAC44 identified the study of the isospin dependence as the highest priority, and conditionally approved the $^{40}_{\Lambda}\text{K}$ and $^{48}_{\Lambda}\text{K}$ measurements as C12-15-008. The Hypernuclear collaboration submitted to PAC 2016 a new proposal on $^{40}_{\Lambda}\text{K}$ and $^{48}_{\Lambda}\text{K}$, mainly focused on the isospin dependence of hyperon dynamics, which was approved.

The recent observation of 2-solar-mass neutron-stars rules out most of the current models for the hyperonic matter equation of state which favour the appearance of hyperons in the neutron star interior but predict maximum masses (M_{max}) incompatible with present data.

This problem, known as the hyperon-puzzle, is presently a subject of very active research. A solution to it necessarily requires a better knowledge of the nuclear interaction involving hyperons. Due to short lifetime of hyperons, the information provided by the available scattering data in the hyperon-nucleon (YN) sector is scarce, and does not allow the determination of the YN interaction using the same scheme successfully employed in the nucleon-nucleon (NN) sector. In the absence of

scattering data, alternative information on the YN interaction can be obtained from hypernuclear physics.

Presently, hypernuclear spectroscopy appears to be the only practical way to study baryonic forces, and may play a significant role towards the solution of the so-called *hyperon puzzle*.

In view of its important astrophysical implications, the extension of the $(e,e'K^+)$ experimental program to a heavy nuclear target with large neutron excess, such as ^{208}Pb , is of primary importance. The study of the $^{208}\text{Pb}(e,e'K^+)$ reaction proposed in this LOI—which will provide information on the properties of a bound hyperon in an environment little affected by surface and shell effects—should be seen as complementary to the measurements to be performed using ^{40}Ca and ^{48}Ca targets, whose main purpose is the analysis of the isospin dependence of hyperon dynamics.

The measured charge density distribution of ^{208}Pb [1] clearly shows that the region of nearly constant density accounts for a very large fraction ($\sim 70\%$) of the nuclear volume, thus suggesting that its properties largely reflect those of uniform nuclear matter in the neutron star interior. The validity of this conjecture has been long established by a comparison between the results of theoretical calculations and the data extracted from the $^{208}\text{Pb}(e,e'p)^{207}\text{Tl}$ cross sections measured at NIKHEF in the 1980s [2,3]

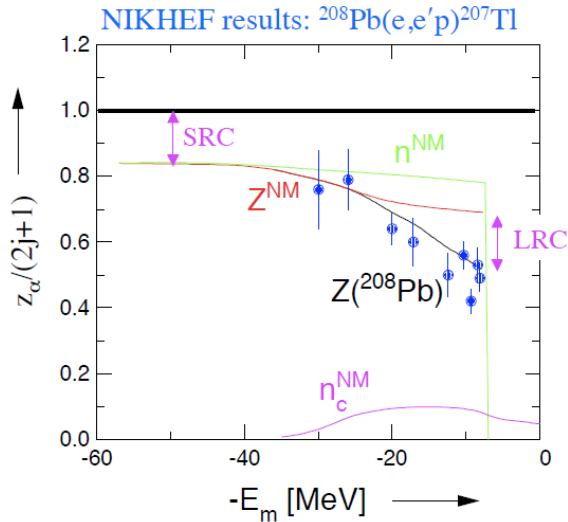


Fig. 1 Energy dependence of the spectroscopic factors extracted from the measured $^{208}\text{Pb}(e,e'p)^{207}\text{Tl}$ cross sections [2,3], compared to the theoretical results of Ref. [4]. The black and red solid lines, labelled $Z(^{208}\text{Pb})$ and Z^{NM} , correspond to ^{208}Pb and uniform nuclear matter, respectively. The effects of short- (SRC) and long-range-correlations (LRC), the latter arising from surface and shell effects, are indicated.

As shown in Fig.1 the energy dependence of the spectroscopic factors, obtained from the analysis of the measured missing energy spectra, turns out to be in remarkably good agreement with the results reported in the pioneering work of Ref. [4]. Short-range correlations appear to be the most important mechanism leading to the observed quenching of the spectroscopic factor, while surface and shell effects only play an important role in the vicinity of the Fermi surface. The picture emerging from Fig. 1 suggests that deeply bound protons in the ^{208}Pb ground state behave as if they were in nuclear matter.

So far, the spectroscopy of heavy hypernuclei has been studied with pion beams and, which do not allow for adequate accuracy and precision. The main issue was the poor resolution, > 2 MeV FWHM. This value turns out to be larger than the 1.8 MeV spacing between the $0i_{13/2}$ and $0h_{9/2}$ neutron-hole states, that produce two series of strongly populated states with the Λ in different orbits. In addition, the spacing between Λ single-particle states is only 4 to 6 MeV. As a result, the existing data do not resolve the two series of states, introducing uncertainties in the theoretical analyses.

The absolute binding energies of all (π^+, K^+) hypernuclear data are based on the 6 events of $^{12}_\Lambda\text{C}$ emulsion data, while in the case of $(e, e'K^+)$ experiments the absolute energy scale can be calibrated exploiting the elementary $p(e, e'K^+)\Lambda/\Sigma^0$ processes. The recent and precise hypernuclear data on $^{10}_\Lambda\text{Be}$ collected at JLab [16]—combined with a careful re-examination of the consistency between emulsion data—point to a possible half-MeV shift of the $^{12}_\Lambda\text{C}$ ground state energy, which would greatly impact on every hypernuclear binding energy measured using the reaction (π^+, K^+) .

Precise hypernuclear spectroscopy on medium to heavy hypernuclei with electron beams, which is only possible with the CEBAF electron beam, is critically important to obtain new information needed to constrain theoretical models of neutron star matter.

The $(e, e'K^+)$ reaction enables the determination of binding energies with high precision because of the calibration provided by the elementary reaction on hydrogen and **is currently the only method that can measure the absolute hypernuclear mass centroids with an unprecedented accuracy of <100 keV**. It provides information on the cross section as well as the binding energy information.

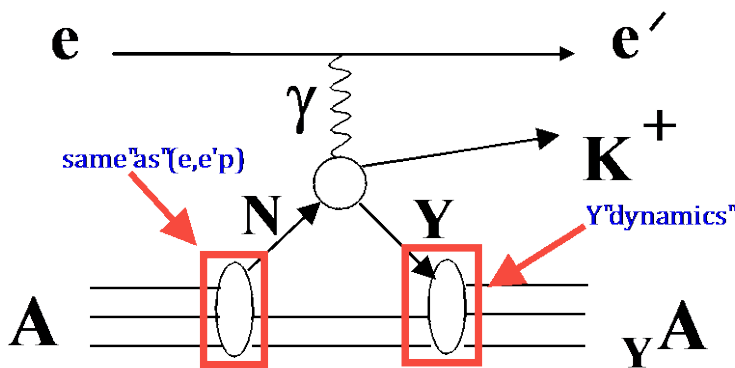


Fig.2 : Schematic representation of the $(e, e'K^+)$ reaction. The left and right boxes highlight the amplitudes involved in the proton and Λ spectral functions, respectively.

Figure 2, provides a schematic representation of the $(e, e'K^+)$ reaction, illustrating the connection with the corresponding $(e, e'p)$ process. The left and right boxes highlight the amplitudes determined by nuclear and hypernuclear dynamics described by the nucleon and hyperon spectral functions respectively.

The availability of the information obtained from the measured $(e, e'p)$ cross sections will be critical for the interpretation of $(e, e'K^+)$ data. To see this, just consider that the hyperon binding energies are given by the difference between the missing energies measured in $(e, e'K^+)$ and the proton binding energies obtained from the $(e, e'p)$ cross sections. Hence, $(e, e'p)$ data will provide the baseline needed to extract information on hyperon binding energies.

Microscopic calculations of the Λ spectral function in a variety of nuclei, ranging from ^5He to ^{208}Pb , have been recently carried out [5]. The results of this analysis—based on a realistic hyperon-nucleon potential model constrained by the available scattering data—suggest that hyperon dynamics in ^{208}Pb may be somewhat different compared to lighter nuclei, as signaled by a larger quenching of the spectroscopic factors.

The results of theoretical calculations of the hyperon spectral function and the wealth of available $^{208}\text{Pb}(e, e'p)$ data—including binding energies and widths of the many proton states—will allow the development of a fully realistic model of the $^{208}\text{Pb}(e, e'K^+)$ cross section, indispensable for the extraction of the information on hypernuclear dynamics.

In view of the above considerations, the use of a ^{208}Pb target appears to be uniquely suited to study Λ interactions in a uniform nuclear medium with large neutron excess

2. Spectroscopic study of heavy hypernuclei through $^{208}\text{Pb}(e,e'\text{K}^+)^{208}\Lambda\text{Tl}$ reaction

The aim of this LOI is to study the $^{208}\text{Pb}(e,e'\text{K}^+)^{208}\Lambda\text{Tl}$ reaction that will provide a better energy resolution than that of the experiments performed so far and thus a more detailed understanding of baryon behavior deep inside of the nucleus, providing important information for studying the Λ single-particle nature under high nucleon density.

We will measure the Binding Energy spectrum of the reaction in Hall A using the HRS spectrometer for electron and the HKS one for kaons.

We will profit of the high quality Jlab electron beam, spectrometers and detectors setup that the hypernuclear collaboration contributed to improve for hypernuclear spectroscopy.

We will use a pure Pb target cooled by cryogenic fluid that will allow to use 25 μA beam and a 100 mg/cm^2 target with reasonable yield and good energy resolution (see Appendix 1)

This is important for many reasons. ^{208}Pb was studied by means of the (π^+, K^+) reaction. The shell structures are barely visible because of the poor energy resolution that doesn't allow to resolve the spectral fine structure, introducing uncertainties into theoretical analyses (see Fig. 3 a).

The good energy resolution of the $(e,e'\text{K}^+)$ reaction will allow a much more precise determination of the Λ single-particle energies to be determined providing besides complementary information with respect to what has been done in the past (and will be done at J-PARC) with hadronic probes. So a precise knowledge of the level structure can, by constraining the hyperon-nucleon potentials, contribute to more reliable predictions regarding the internal structure of neutron stars and in particular their maximum mass.

The experiments we propose can have good statistics and sufficient resolution to separate at least the major shell states from those configuration mixing states as seen in the Hall C $^{28}\Lambda\text{Al}$ spectrum [17]. The more accurate information on the binding energies and spacing of the Λ single-particle states in heavy nuclei (the ^{40}Ca and ^{48}Ca approved by PAC and ^{208}Pb we are proposing in this LOI) will provide an anchor point for the systematics of Λ single-particle states across the periodic table.

2.1 The proposed experiment

The aim of the experiment is measuring the $^{208}\text{Pb}(e,e'\text{K}^+)^{208}\Lambda\text{Tl}$ reaction. Fig. 3b shows the missing mass spectrum obtained by the $^{208}\text{Pb}(\pi^+, \text{K}^+)^{208}\Lambda\text{Pb}$ reaction as calculated by Motoba and Millener using SLA elementary amplitudes [6]. It shows a characteristic bump structure starting from the binding energies B_Λ around 25 MeV.

The experiment will make it possible to determine with much better precision the binding energy (thanks to the calibration achievable exploiting the elementary $p(e,e'\text{K}^+)\Lambda/\Sigma^0$ processes with hydrogen), and to test both the dynamical models and the computational techniques employed in the available theoretical approaches.

Spectroscopic data exist for few Λ hypernuclei obtained through the $(e,e'\text{K})$ reaction spectroscopy and few others would be available with the presently approved experiment. Consequently it is extremely important to perform $(e,e'\text{K})$ experiment also on ^{208}Pb . The much better energy resolution of binding energy spectra of hypernuclei generated through $(e,e'\text{K})$, a factor of ~ 3 (see Fig 3a and 3b) better than in spectra of hypernuclei generated with π , K probes, will allow the determination of much more precise Λ single-particle energies..

This will allow us to test different theoretical models.

It will be possible to “see” deep shells, in practice not visible with (π, K) reaction (“the observed small peaks *are assumed* to be the $s\Lambda$ states” [7])

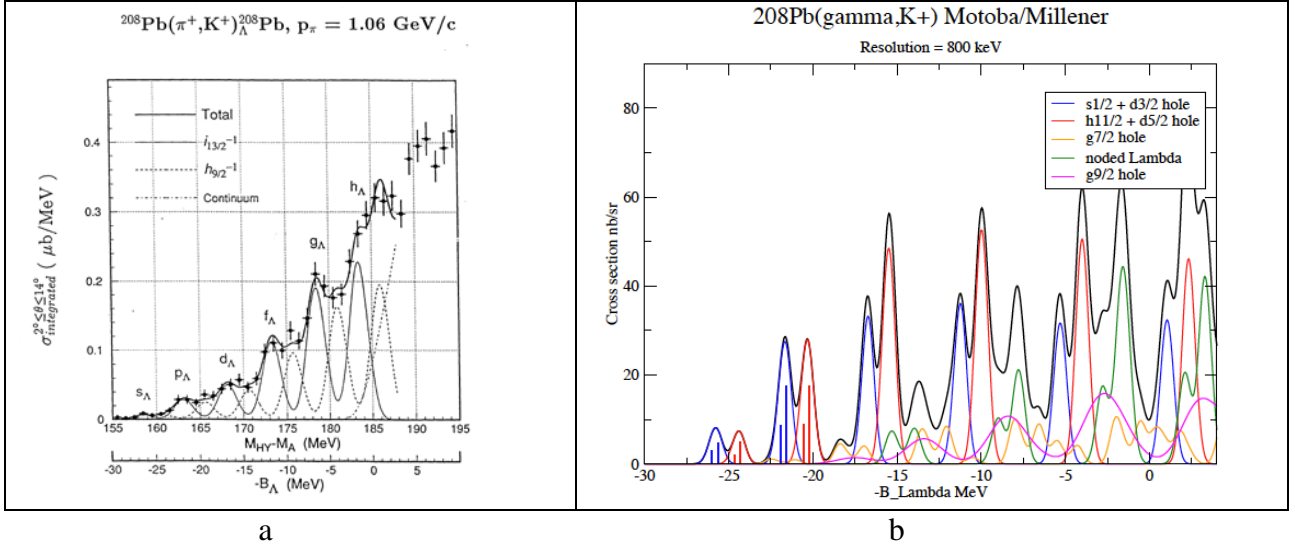


Fig. 3 a. Missing mass spectrum of ^{208}Pb measured in E140 experiment b. ^{207}Tl core nucleus level scheme

Fig. 3b shows the Binding Energy Spectrum expected for $^{208}\text{Pb}(\gamma, K^+)^{208}\Lambda\text{Tl}$ calculated for our kinematics using the Saclay Lyon [6] elementary amplitudes. The Λ is assumed to be weakly coupled to the proton-hole states of ^{207}Tl strongly populated in (e,e'p) or (d,3He) reactions on ^{208}Pb . The Λ single-particle energies were calculated from a Woods-Saxon well fitted to energies derived from the $^{208}\text{Pb}(\pi, K^+)^{208}\Lambda\text{Pb}$ reaction. Just a few states cannot be resolved : states based on the closely-spaced p $2s_{1/2}^{-1}$ and p $1d_{3/2}^{-1}$ states cannot be resolved (blue bars and curves). Likewise for the p $0h_{11/2}^{-1}$ and p $1d_{5/2}^{-1}$ states cannot be resolved (red bars and curves). The successive red and blue peaks correspond to the population of the $0s$, $0p$, $0d$, $0f$, $0g$, and $0h$ Lambda orbits. The green lines correspond to the noted $1s$, $1p$, $1d/2s$, and $1f$ Λ orbits. The remaining 5 curves correspond to strength based on deeper and fragmented proton-hole strength.

The Λ binding energy extracted from the measured cross sections will provide most valuable new information, needed to constrain the models of hyperon interactions in nuclear

2.2 Beam time requirement

Calculations in the Appendix 1 show that 4-5 weeks of beam time will be sufficient to measure the spectrum shown in Fig. 3 b

3. Summary and conclusions

The experiment on ^{208}Pb described in this LOI, is an essential part of the campaign of measurements the Jefferson Lab hypernuclear collaboration is doing.

The study of the $^{208}\text{Pb}(e, e'K^+)^{208}\Lambda\text{Tl}$ reaction together with the other reactions proposed to this PAC by the same collaboration will “complete” the systematic study of Λ hypernuclear bound states over the wide mass range. Moreover, it will provide significance new information, much needed to constrain the available theoretical models of neutron star matter, and shed light on the so-called *hyperon puzzle*.

Appendix 1

1. The target

A major concern is developing a Pb target that could operate at high beam currents without melting. We considered different options:.

a. A 0.5 mm of Lead has to be sandwiched between two 0.15 mm of diamond that is pure ^{12}C as done by the PREX experiment [31] (see Fig. 6). This would allow to run with $\sim 70 \mu\text{A}$ on a $100 \text{ mg}/\text{cm}^2$ (or thicker, but degradation of energy resolution would happen). The major drawback of this option would be the Excitation Energy spectrum highly contaminated by the Carbon spectrum.

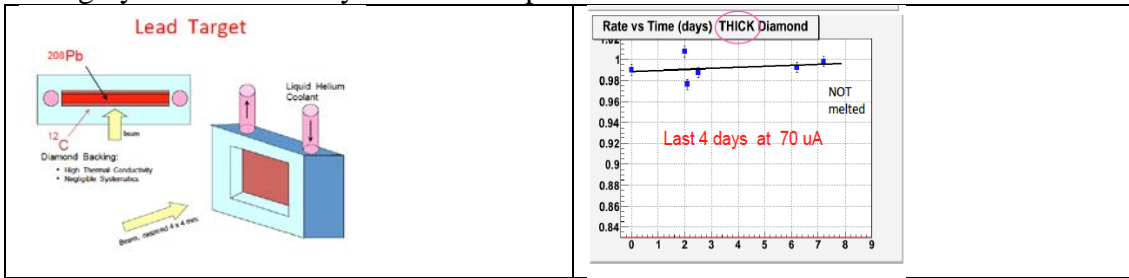


Fig. 4 The PREX Lead target.

Performance of one of the PREX targets

b. The setup used at NIKHEF for (e,e'p) experiment [Ref. 3, and C. Marchand, personal communication]. This would allow to run safely with $10 \mu\text{A}$ of beam current and $100 \text{ mg}/\text{cm}^2$ (or thicker) of pure ^{208}Pb target

c. The same setup as at point "b" but cooling with a cryogenic liquid to allow to use with higher beam currents ($\sim 25 \mu\text{A}$) to be able to increase the counting rate so improving the "detectability" of the small peaks.

After considering the options b and c and discussing with JLab target group, we decided to adopt the solution

c.

The Fig. 5 shows the layout of the NIKHEF layout of the $\sim 100 \text{ mg}/\text{cm}^2$ pure Pb target [3].

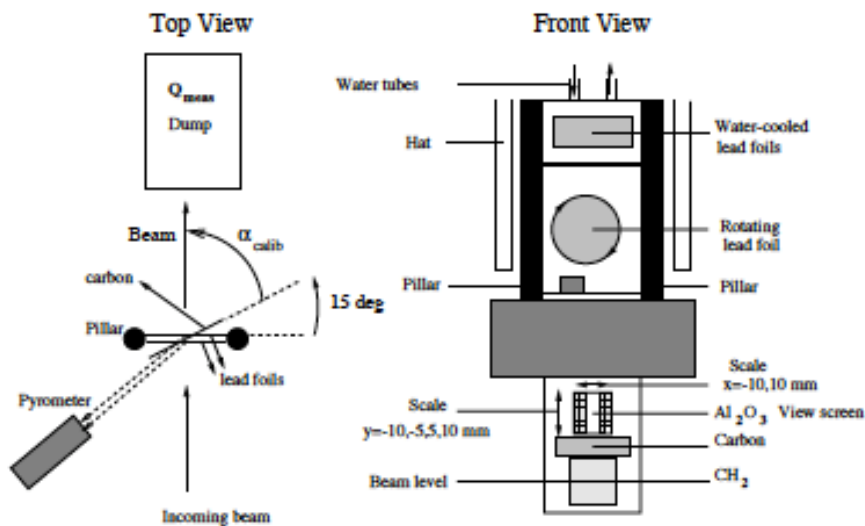


Fig. 5 The NIKHEF ^{208}Pb target layout

The beam current was $10 \mu\text{A}$. To avoid melting the target was cooled by a water flow ($15 \text{ }^\circ\text{C}$) of up to $95 \text{ dm}^3/\text{h}$ during the actual data taking.

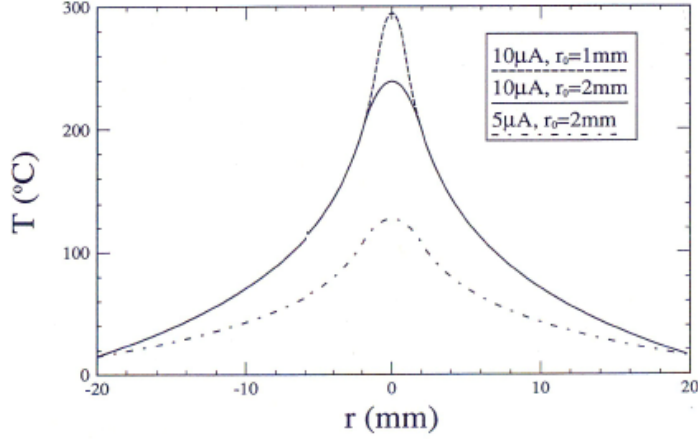


Fig.6. Temperature profile of a circular water cooled lead target of radius 20 mm. The dashed curve corresponds to 10 μ A beam spot of 1 mm radius, the solid curve to a 10 μ A beam spot of 2 mm radius. And the dot-dashed curve to a 5 μ A beam spot of 2 mm radius.

Heat transfer calculation show that conduction cooling becomes competitive as compared to increased radiation cooling by rotating or wobbling the target for thick targets. The computed temperature profile caused by a beam spot of radius r_0 on a circular target of radius r_1 is shown in Fig. 6.

For our experiment we plan to use cryogenic fluid to cool the target. The maximum current one can use without melting the target can be calculated by the formula

$$\langle i_{\max} \rangle = 2\pi k (T_{\text{melting}} - T_0) / \{ [\ln(r_1/r_0) + 1/2] \rho dE/dx \}$$

where $\langle i \rangle$ is the beam current, $k \sim 35.3 \text{ W.K}^{-1}.\text{m}^{-1}$, dE/dx the energy loss of the electrons in the target per unit length ($1.55 \text{ MeV.g}^{-1}.\text{cm}^2$, $\rho \sim 11.35 \text{ g/cm}^3$ for lead, T_{melting} is 601K for lead. This shows that using cryogenic cooling we can use a beam current of $\sim 35 \mu\text{A}$. However, the actual shape of the target is not circular, neither is the exact shape and size of the beam spot known. Therefore what shown in the Fig. 8 gives only a first order estimation of the expected heat dissipation performance. For this reason we assume, conservatively, that we can run with 25 μA . Tests will be performed to check if a current as high as 35 μA could be used.

We will setup a system that allows to monitor continuously the target thickness when is exposed to beam. At Nikhef the temperature was monitored by a pyrometer setup. This instrument measured a temperature of 394-414 K during the experiment which was conveniently below the melting temperature of lead (601 K). The position of this instrument is shown in Fig.6.

For our experiment we plan to monitor the target thickness by performing elastic scattering measurement off Pb-208 to know the actual thickness of the target at the first stage of the beamtime. During data taking, we will monitor continuously the thickness of the target by measuring electron scattering rate as a function of two-dimensional positions by using raster information. This method was already used for CH_2 target in Hall-C hypernuclear programs and cracking or melting of the target were monitored to know right time for target exchange.

2. Particle Identification

The identification of kaons detected in the hadron arm together with a huge background of protons and pions is one of the major challenge of the experiment. To reduce the background level in produced spectra, a very efficient PID system is necessary for unambiguous kaon identification. In the electron arm, the Gas Cherenkov counters [12] give pion rejection ratios up to 10^3 . The dominant background (knock-on electrons) is reduced by a further 2 orders of magnitude by the lead glass shower counters, giving a total pion rejection ratio of 10^5 . The lead-glass shower counters and the gas Cherenkov are calibrated against each other.

The PID system in the hadron arm of HKS is composed of: three planes of time-of-flight counters, two planes of water Cerenkov counters, and three planes of aerogel Cerenkov counters. The power rejection capability is:

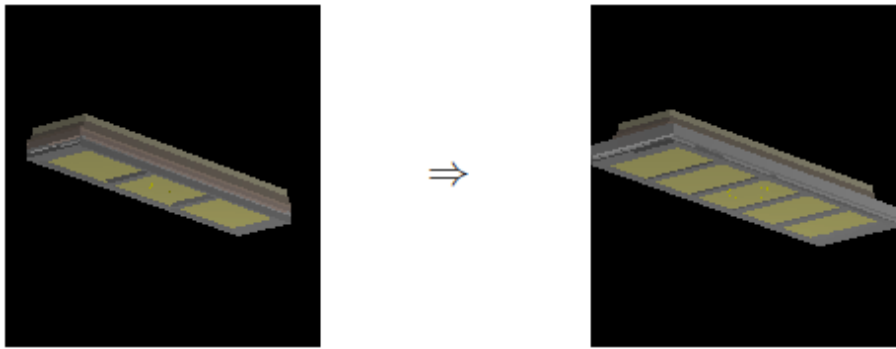
- In the beam π :K:p 10000:1:2000

- in the on-line trigger 90:1:90
- after off-line analysis it is 0.01:1:0.02
- so for π the rejection power is 10^6
- and for proton 10^5

The Hall A RICH detector will be added to improve the kaon identification. The detector [27,28,29] was used successfully during the E-94-107 experiment providing a very good pion/kaon rejection at 2 GeV/c better than 1:1000 (corresponding to a pion/kaon angle separation of ~ 6.0 sigma) [13,14,15].

The layout of the RICH is conceptually identical to the ALICE HMPID design. It uses a proximity focusing geometry, a CsI photocathode, and a 15 mm thick liquid Freon radiator. A detailed description of the layout and the performance of the detector is given in [13,14,15]. After the E-94-107 experiment the detector was upgraded to match the needs of the Transversity approved experiment (E06-011) to be able to identify kaons of 2.4 GeV/c. The upgrade extended the performance by means of a larger photon detector (a multiwire-multipad proportional chamber) and a longer proximity gap which improved the photon detection geometrical efficiency and the angular resolution, respectively.

Upgraded Proximity Focusing RICH @ JLab



| | |
|-------------------|---|
| Radiator | 15 mm thick Liquid Freon (C_6F_{14} , $n=1.28$) |
| Proximity Gap | 100 \rightarrow 175 mm, filled with Methane at STP |
| Photon converter | 300 nm CsI film coated on Pad Planes |
| Position Detector | 3 \rightarrow 5 \times pad planes = 1940 \times 403 \rightarrow 2015 \times 646 mm ² |
| | Multi Wire/Pad Proportional Chamber, HV= 1050 \div 1100 V |
| Pad Plane | 403.2 \times 640 mm ² (single pad: 8.4 \times 8 mm ²) |
| FE Electronics | 11520 \rightarrow 19200 analog chs. multiplexed S&H  |

Fig. 7 Old and new upgraded RICH layout

In Fig. 7 we show the old and new (upgraded) layout. The photon detection plane were nearly doubled (3 more pad panels added). This would have allowed the detectors to separate kaons, in the E-94-107 kinematical conditions (at a kaon momentum ~ 2 GeV/c) with a higher rejection ratio, an additional ~ 1.5 sigma (Fig.8,9) corresponding to a pion:kaon rejection better than 1:10000 at 2.0 GeV/c, with improved efficiency.

In our experiment the central momentum of the detected kaons will be 1.2 GeV/c. For this reason even better performances to separate kaons from pions will be obtained. Easy calculation [13,14,15] provide an estimate of ~ 7.8 sigma the pion – kaon Cherenkov separation angle. Adding conservatively 1.5 sigma, we would obtain a separation ~ 9.3 sigma. This would correspond to a $\sim 10^6$ power rejection

Convoluting the threshold Cherenkov and the RICH power rejection we would have a pion-kaon power rejection $\sim 10^{12}$

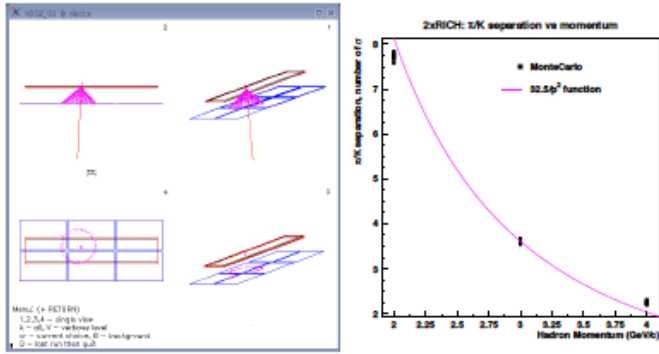


Fig. 8 Upgraded RICH simulation events (left panel) and expected performance (right panel): pion-kaon separation (number of sigmas) at different hadron momenta. The simulation is tuned to the E-94-107 hypernuclear experimental data.

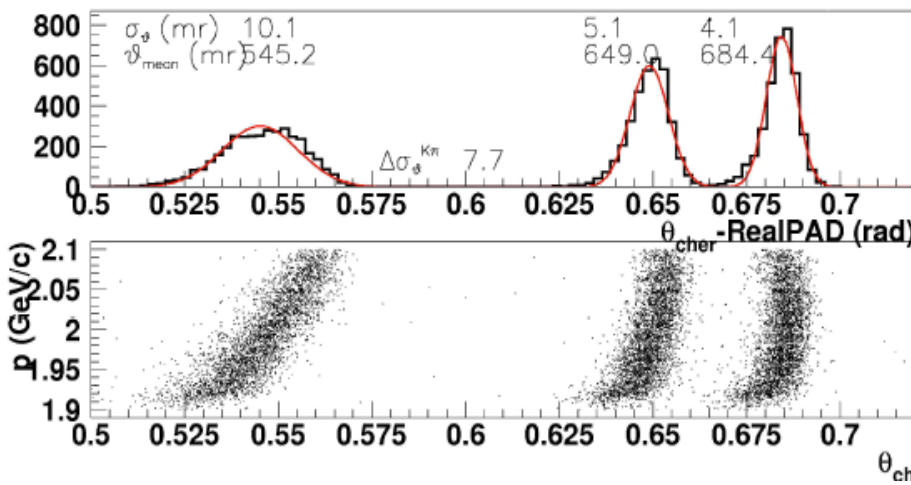


Fig.9 Upgraded RICH simulated performance. From left to right Pion/Kaon angle distribution (equal hadrons populations) at 2 GeV/c momentum, in the HRS acceptance. The Montecarlo is tuned on Hall A hypernuclear experimental data.

3. Kinematics and counting rates

3.1 Kinematics

The definition of the kinematics angles and their limits are illustrated in Fig. 10. This design is based on the kinematics using a 4.5238 GeV beam, minimum HRS angle when using a Septum for an e^- momentum at ~ 3 GeV/c, and maximization of overlap of the virtual photon angular range and the HKS angular coverage to promote the highest possible production yield, while having a sufficiently large separation to completely avoid the forward scattered electrons and positrons.

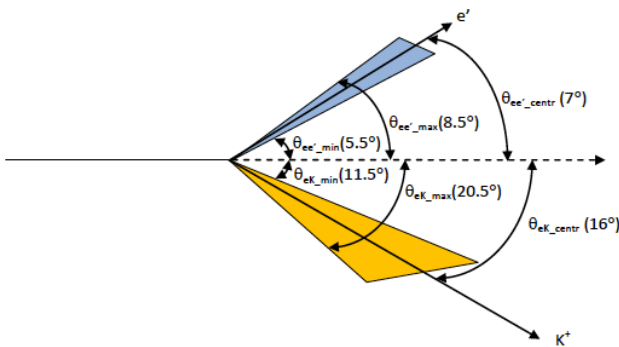


Fig. 10 Kinematics

The kinematics parameters and ranges are listed in Table 2. A GEANT simulation taking into account the realistic and known conditions of HRS and HKS was performed. No acceptance limitation was included for the new Septum magnets which do not yet have detailed engineering design. Details can be found in Chapter 2 (Experimental Methods etc).

Table 2 Basic kinematics parameters of the Septum+HRS and Septum+HKS system

| | |
|--|---|
| Beam energy (12 GeV mode, 2-passes, injector energy included) | 4.5238 GeV |
| E' (HRS) central angle (horizontal and vertical bites) | 7° ($\pm 1.5^\circ$ and $\pm 2.5^\circ$) |
| E' (HRS) central momentum (percentage bite) | 3.0296 GeV/c ($\pm 4.5\%$) |
| Virtual photon central angle ($\phi=\pi$) | 13.68° |
| Virtual photon energy range | 1.35 – 1.62 GeV |
| Virtual photon momentum range | 1.40 – 1.70 GeV/c |
| Average Q^2 | -0.218 (GeV/c) ² |
| K ⁺ (HKS) central angle (horizontal and vertical bites) | 16° ($\pm 4.5^\circ$ and $\pm 2.5^\circ$) |
| K ⁺ (HKS) central momentum (percentage bite) | 1.2 GeV/c ($\pm 12.5\%$) |
| Lab $\theta_{\gamma K}$ coverage range | 0° - 9° |

3.2 Counting rates

Fig. 11 shows the ²⁰⁷Tl core nucleus level scheme. Table 3 shows the spectroscopic factors measured in ²⁰⁸Pb(d, ³He)²⁰⁷Tl reaction. They are large enough for many low-lying states of ²⁰⁷Tl core nucleus (up to excitation energy ~4 MeV) and that the corresponding hypernuclear states with a Λ coupled to these core states are populated.

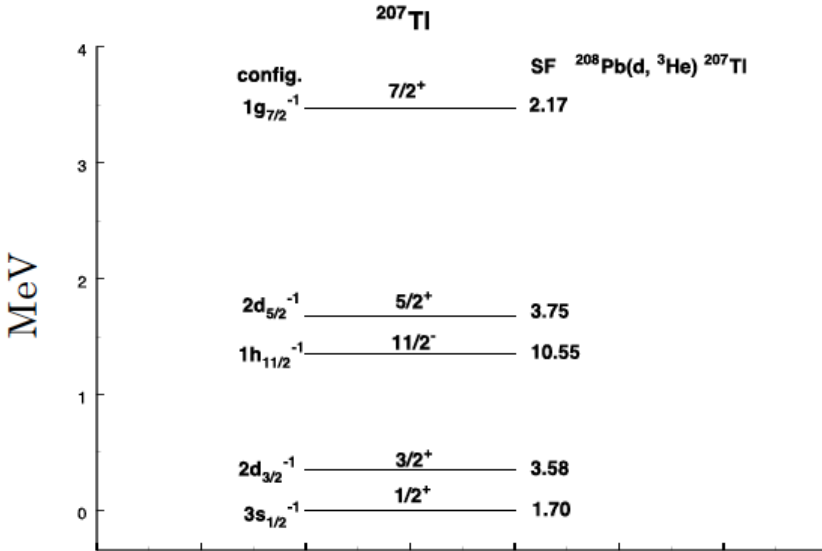


Fig. 11 ²⁰⁷Tl energy spectrum, dominant configurations and spectroscopic factors

Fig. 3b shows the spectrum for ²⁰⁸Pb(γ , K⁺)²⁰⁸ Λ Tl calculated for our kinematics using the Saclay Lyon elementary amplitudes with assumed resolution of 500 keV (FWHM). The Λ is assumed to be weakly coupled to the proton-hole states of ²⁰⁷Tl that are strongly populated in the (e, e'p) or (d, ³He) reactions on ²⁰⁸Pb. The Λ

single-particle energies were calculated from a Woods-Saxon well fitted to energies derived from the $^{208}\text{Pb}(\pi^+, \text{K}^+)^{208}_{\Lambda}\text{Pb}$ reaction. States based on the closely-spaced p $2s_{1/2-1}$ and p $1d_{3/2-1}$ states are

Table 2

^{207}Tl energy spectrum, dominant configurations and spectroscopic factors.

| E_x MeV | J^π | Config. | C^2S |
|-----------|---------|------------------|--------|
| 0.000 | 1/2+ | $2s_{1/2}^{-1}$ | 1.70 |
| 0.351 | 3/2+ | $1d_{3/2}^{-1}$ | 3.58 |
| 1.348 | 11/2- | $0h_{11/2}^{-1}$ | 10.6 |
| 1.683 | 5/2+ | $1d_{5/2}^{-1}$ | 3.75 |
| — | — | — | — |
| 3.747 | 7/2+ | $0g_{7/2}^{-1}$ | 2.17 |

Using the Sotona and Millener - Motoba calculations and extrapolating from precedent experiment on ^{12}C the electron, pion and kaon single rates and hypernuclei, as well as the beam time needed for the experiment were evaluated. The cross-section is \sim six times lower than the same reaction on ^{12}C target. The rate of K^+ and the rate of background hadrons in HKS as function of Z and A are known and measured. We estimated the coincidence counting rate for signal and background, assuming a rate of electrons in HRS to be comparable to the value measured in the E94-107 experiment for the same weighted thickness and beam current. This is confirmed by calculation and test measurement performed in Hall A for Apex experiment [Ref. Bogdan Wojtsekhowski, personal communication]. In Table 3 we show the single and coincidences rates for ^{208}Pb as function of the target thickness and beam current. The Signal to Noise ratio is also evaluated for the first 4 peaks (s shell and p shell). We show the Signal to Noise Ratio (Peak significance) defined as $S/\sqrt{S+B}$, where S is the signal (integrated number of counts above the background in the peak) and B the background number of counts below the peak. It should be noted that, due to the large background, the Signal to Noise ratio doesn't improve too much increasing the target thickness. For this reasons we plan to use a current as high as 25 μA and a target thickness of 100 mg/cm^2 . Tests will be performed to check if a current as high as 35 μA could be used. This target thickness in principle allows to obtain an energy resolution \sim 550 keV or better (see Chapter 2. Experimental Methods). However, conservatively, we will assume an Energy resolution of \sim 800 keV.

Table 3

| Thickness (mg/cm ²) | <I> (μ A) | (e,e') (kHz) | (e,k') (kHz) | (e,p') (kHz) | Accid. (Hz) (e,e')(e,k') Δ t | Backgnd (c/h/MeV) | Coincidence Z(e,e'K)Z-1 (c/h) | Peak Significance | Peak |
|------------------------------------|-------------------|-----------------|-----------------|-----------------|--|----------------------|-------------------------------------|----------------------|--------------|
| 100 | 25 | 37 | 0.07 | 16 | 0.01 | 0.10 | 0.06 | 4.3 | s-shell g.s. |
| 200 | 25 | 75 | 0.14 | 32 | 0.04 | 0.38 | 0.12 | 4.7 | s-shell g.s. |
| 300 | 25 | 113 | 0.21 | 47 | 0.10 | 0.86 | 0.19 | 4.9 | s-shell g.s. |
| 100 | 25 | 37 | 0.07 | 16 | 0.01 | 0.10 | 0.21 | 10.5 | p-shell g.s. |
| 200 | 25 | 75 | 0.14 | 32 | 0.04 | 0.38 | 0.41 | 12.8 | p-shell g.s. |
| 300 | 25 | 113 | 0.21 | 47 | 0.10 | 0.86 | 0.62 | 14.0 | p-shell g.s. |
| 100 | 35 | 52 | 0.10 | 22 | 0.02 | 0.19 | 0.09 | 4.4 | s-shell g.s. |
| 200 | 35 | 105 | 0.20 | 44 | 0.08 | 0.75 | 0.17 | 4.9 | s-shell g.s. |
| 300 | 35 | 157 | 0.30 | 66 | 0.19 | 1.68 | 0.26 | 5.1 | s-shell g.s. |
| 100 | 35 | 52 | 0.10 | 22 | 0.02 | 0.19 | 0.29 | 11.6 | p-shell g.s. |
| 200 | 35 | 105 | 0.20 | 44 | 0.08 | 0.75 | 0.58 | 13.6 | p-shell g.s. |
| 300 | 35 | 157 | 0.30 | 66 | 0.19 | 1.68 | 0.88 | 14.6 | p-shell g.s. |

Actually we cannot resolve the g.s. so we will have to sum up the first two levels. The same for the p shell peaks and so on.

The calculations in Tab3 assume a beam time request of 840 hours (5 weeks). The calculation of the background has been extrapolated to the measured values of the precedent experiment on a ¹²C target (see text in the main part)

References

1. B. Frois and C. N. Papanicolas, Ann. Rev. Nucl. Part. Sci. **37**, 133 (1987).
2. E. N. Quint et al., Phys. Rev. Lett. **56**, 186 (1986); E. N. Quint et al., Phys. Rev. Lett. **58**, 1727 (1987).
3. M. van Batenburg, PhD Thesis, University of Utrecht, 1996.
4. O. Benhar, A. Fabrocini, and S. Fantoni, Phys. Rev. C **41**, R24 (1990).
5. I. Vidaña, Nucl. Phys. **958**, 468 (2017).
6. J.C. David, C. Fayard, G.-H. Lamot, B. Saghai, **Phys. Rev. C** **53**, 2613 (1996);
T. Mizutani, C. Fayard, G.-H. Lamot, B. Saghai, **Phys. Rev. C** **58**, 75 (1998).
7. "Spectroscopy of Λ hypernuclei," Review paper, O. Hashimoto and H. Tamura,
Progress in Particle and Nuclear Physics 57 (2006).
8. T. Hasegawa et al, Phys. rev C53 (1996) 1210
9. C.B. Dover, Proc. Int. Sympto. on Medium Energy Physics, Beijing. World Scientifics, Singapore,
1987, p. 257
10. F. Garibaldi, S. Frullani, P. Markowitz and J. LeRose, spokespersons, JLab proposal for E94-107.
11. F. Cusanno et al, Phys. Rev. Lett. 103, 202501 (2009).
12. J. Alcorn et al. Nucl. Instr. and Methods A 522, 294 (2004)
13. M. Iodice et al., Nucl. Instr. and Methods A 553, 231 (2005)

14. F.Garibaldi et al., Nucl. Instr. and Methods A 502, 117 (2003)
15. F. Cusanno et al., Nucl. Instr. And Methods A 502, 251 (2003)
16. T.Gogami et al., PRC 2016, DOI 10.1103/PhysRevC.93.034314)
17. S.N.Nakamura, T.Gogami, L.Tang et al., Proceeding of the 12thInternational Conference on Hypernuclear and Strange Particle Physics (HYP2015), JPS Conference Proceedings, in press.